FACE DETECTION AND RECOGNITION USING OpenCV AND FACE REGOGNITION LIBRARIES IN PYTHON

A PROJECT REPORT

Submitted by

ANJHANA M [Reg No:RA2111003011478]

JOLLY M [Reg No: RA2111003011453]

DEVANGANA B [Reg No:RA2111003011454]

DIYA GURJAR [Reg No: RA2111003011449]

RAAJ SURYA A [Reg No: RA2111003011425]

RIYA AGARWAL [Reg No: RA2111003011420]

Under the Guidance of

Dr. SHOBA LK

Associate Professor, Department of Computing Technologies

in partial fulfillment of the requirements for the degree of

BACHELOR OF TECHNOLOGY

in

COMPUTER SCIENCE AND ENGINEERING

DEPARTMENT OF COMPUTING TECHNOLOGIES

COLLEGE OF ENGINEERING AND TECHNOLOGY

SRM INSTITUTE OF SCIENCE AND TECHNOLOGY

KATTANKULATHUR– 603 203

NOVEMBER 2023

SRM INSTITUTE OF SCIENCE AND TECHNOLOGY
KATTANKULATHUR–603 203

BONAFIDE CERTIFICATE

Certified that 18CSP109L / I8CSP111L project report titled "**FACE DETECTION AND RECOGNITION USING OpenCV AND FACE REGOGNITION LIBRARIES IN PYTHON** is the bonafide work of **ANJHANA M[RegNo:RA2111003011478], JOLLY M[RegNo:RA2111003011453], DEVANGANA B[RegNo:RA2111003011454]** , **DIYA GURJAR[RegNo:RA2111003011449]**, **RAAJ SURYA A[RegNo:RA2111003011425], RIYA AGARWAL[RegNo:RA2111003011420]** who carried out the project work under my supervision. Certified further, that to the best of my knowledge the work reported here does not form part of any other thesis or dissertation based on which a degree or award was conferred on an earlier occasion for this or any other candidate.

Dr. SHOBA LK
SUPERVISOR
Assistant Professor
Department of Computing Technologies

Dr. M. PUSHPALATHA
HEAD OF THE DEPARTMENT
Department of Computing Technologies

Department of Computing Technologies

SRM Institute of Science and Technology
Own Work Declaration Form

Degree/Course : B.Tech in Computer Science and Engineering
Student Names : ANJHANA M, JOLLY M, DEVANGANA B, DIYA GURJAR, RAAJ SURYA A , RIYA AGARWAL
Registration Number: RA2111003011478, RA2111003011453, RA2111003011454, RA2111003011449, RA2111003011425, RA2111003011420.

Title of Work : FACE DETECTION AND RECOGNITION USING OpenCV AND FACE REGOGNITION LIBRARIES IN PYTHON

I/We here by certify that this assessment compiles with the University's Rules and Regulations relating to Academic misconduct and plagiarism, as listed in the University Website, Regulations, and the Education Committee guidelines.
I / We confirm that all the work contained in this assessment is our own except where indicated, and that we have met the following conditions:

- Clearly references / listed all sources as appropriate, Referenced and put in inverted commas all quoted text (from books, web,etc.)
- Given the sources of all pictures, data etc that are not my own.
- Not made any use of the report(s) or essay(s) of any other student(s)either past or present, Acknowledged in appropriate places any help that I have received from others (e.g fellow students, technicians, statisticians, external sources)
- Compiled with any other plagiarism criteria specified in the Course hand book / University website

I understand that any false claim for this work will be penalized in accordance with the University policies and regulations.

DECLARATION:
I am aware of and understand the University's policy on Academic misconduct and plagiarism and I certify that this assessment is my / our own work, except where indicated by referring, and that I have followed the good academic practices noted above. **Date:14/11/23**
Student 1 Signature: ANJHANA M **Student 2 Signature: JOLLY M** **Student 3 Signature: DEVANGANA B** **Student 4 Signature: DIYA GURJAR** **Student 5 Signature: RAAJ SURYA A** **Student 6 Signature: RIYA AGARWAL**

ACKNOWLEDGEMENT

We express our humble gratitude to **Dr. C. Muthamizhchelvan**, Vice-Chancellor, SRM Institute of Science and Technology, for the facilities extended for the project work and his continued support.

We extend our sincere thanks to Dean-CET, SRM Institute of Science and Technology, **Dr. T. V. Gopal**, for his invaluable support.

We wish to thank **Dr. Revathi Venkataraman**, Professor and Chairperson, School of Computing, SRM Institute of Science and Technology, for her support throughout the project work.

We are incredibly grateful to our Head of the Department, **Dr. M. Pushpalatha,** Professor, Department of Computing Technologies, SRM Institute of Science and Technology, for her suggestions and encouragement at all the stages of the project work.

We register our immeasurable thanks to our Course Faculty, **Dr. SHOBA LK**, Assistant Professor, Department of Computing Technologies, SRM Institute of Science and Technology, for leading and helping us to complete our course.

ANJHANA M[RegNo:RA2111003011478]
JOLLY M[RegNo:RA2111003011453]
DEVANGANA B[RegNo:RA2111003011454]
DIYA GURJAR[RegNo:RA2111003011449]
RAAJ SURYA A[RegNo:RA2111003011425]
RIYA AGARWAL[RegNo:RA2111003011420]

ABSTRACT

This project explores the development of an advanced face detection and recognition system using OpenCV and dedicated face recognition libraries in Python. The study delves into the theoretical foundations of image processing, feature extraction, and machine learning algorithms crucial for effective face detection and recognition. Leveraging the versatile OpenCV library and specialized tools like the Face Recognition library, which utilizes dlib and deep learning techniques, the project establishes a comprehensive system architecture. This architecture encompasses the entire face detection pipeline, feature extraction methods, and the integration of machine learning models for recognition. Practical experiments and evaluations with diverse datasets assess the system's accuracy, speed, and reliability, revealing its efficacy in handling challenging scenarios such as variable lighting and pose variations. The results contribute to the evolving landscape of computer vision applications, demonstrating the system's potential in security, human-computer interaction, and personalized user experiences. The project concludes with recommendations for future enhancements, providing a foundation for continued advancements in face detection and recognition technologies.

In addition to its technical contributions, this project also emphasizes the ethical considerations associated with face detection and recognition systems. Privacy concerns, potential biases, and the responsible deployment of such technologies are discussed. The report highlights the importance of incorporating fairness and transparency in algorithmic decision-making processes, aiming to address societal implications and ensure equitable outcomes. By recognizing the ethical dimensions, the project not only advances the technical aspects of face detection and recognition but also underscores the necessity of responsible development and deployment practices in the broader context of artificial intelligence. This multi-faceted approach contributes to a more holistic understanding and responsible application of face detection and recognition systems in real-world scenarios.

TABLE OF CONTENTS

LIST OF TABLES

LIST OF FIGURES

CHAPTER 1

INTRODUCTION
CHAPTER I

The automatic detection of facial landmarks is a crucial aspect of face recognition research, widely used in various fields, including facial surgeries, biometrics, information security, access control for law enforcement, surveillance systems, and smart cards.

Current solutions for facial landmark detection mostly work on 2D images (photos). However, as 3D images (scans) become more prevalent due to recent advances in technologies and affordability, research on automatically detecting facial landmarks on 3D images is gaining interest among researchers. Using 3D images for facial landmark detection has the potential to overcome challenges faced when using 2D images, such as variations in lighting, posture, expression, and occlusion. The techniques used in the field of facial landmark detection on 3D images have been categorized in various ways by researchers. One recent categorization divides the techniques into two main categories: conventional and deep learning methods.

Conventional techniques can be further divided into three subcategories: local feature-based, holistic-based, and hybrid. Local-based approaches focus on specific facial features, such as the nose and eyes, while holistic-based approaches use the entire face to generate feature vectors for landmark detection. Hybrid methods combine both local and global facial features. For conventional methods, the key step is finding robust feature points and descriptors based on the geometric information of 3D face data. Conventional methods for facial landmark detection also utilize statistical feature models in addition to geometric information. The related work that focuses on geometric information employs four types of methods: curvature analysis, combining 2D texture with 3D shape, matching 3D face templates with a manually marked model to establish correspondences, and using generic image descriptors.

On the other hand, deep learning methods have been used to provide solutions to find facial landmark locations on 3D images. A common approach to facial landmark detection on 3D scans is to use a 3D CNN (Convolutional Neural Network) which consists of 3D convolutional kernels and 3D pooling layers. Another approach is to use a combination of a 2D CNN and a 3D morphable model (3DMM). This method uses the 2D

CNN to predict 2D landmark locations on an image of the face, which is then used to fit a 3DMM and estimate the 3D landmark positions.

Machine Learning (and hence deep learning) is recommended to solve complex problems for which using a traditional approach yields no good solution

We believe geometric properties of the face embedded in the 3D face scans can be utilized to accurately locate some of the facial landmarks. Several studies have demonstrated the effectiveness of utilizing geometric and statistical features in facial landmark detection. For instance, Abu et al. Gupta et al.

, Vezzetti et al. Liang et al., Li et al. and Manal et al.have successfully detected 8, 10, 13, 17, 25, and 30 landmarks, respectively. In this study, we build upon the existing work utilizing the geometric properties of facial features on 3D models.

We reviewed the literature and developed algorithms for thirty-eight landmarks utilizing geometric properties and statistical information about facial measurements. Eight of our algorithms were based on existing work, while thirty were original contributions. The implementation of these algorithms is provided as open-source Python code, along with the pseudocode for both our algorithms and those found in the literature. To the best of our knowledge, this study covers the most extensive number of facial landmark detection algorithms based on the geometric properties of 3D models. The accuracy of the algorithms was evaluated using over a hundred 3D facial scans.

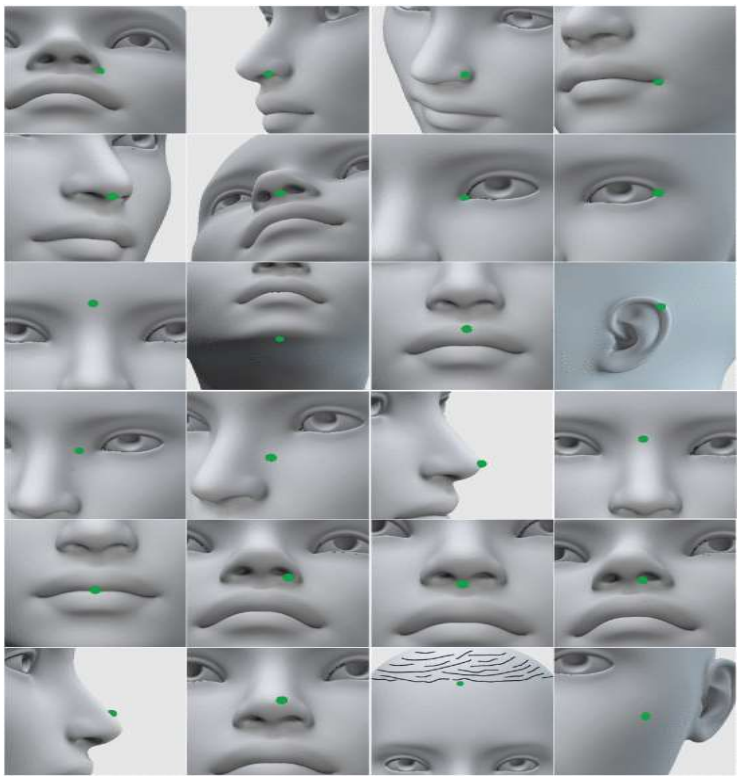

METHODS AND MATERIALS

CHAPTER II

Facial features (landmarks) and measurements that are in use by researchers and facial plastic surgeons were presented in a recent literature review article [20] and a free web-based facial analysis tool [21]. While there are over a hundred facial landmarks, we focused on the ones that are more relevant to facial plastic surgery. We consulted with surgeons and asked which measures (distances, angles, and ratios) are most important for facial plastic surgeries, specifically rhinoplasty. Based on their answers, we identified landmarks and also added landmarks that are used for computing visualization about facial symmetry such as endocanthion and exocanthion. Fourteen of the landmarks are bilateral, meaning that they exist on both the left and right sides of the face symmetrically. The total number of facial landmarks adds up to thirty-eight. Figure 1 shows the facial landmarks that we study. The bilateral landmarks are only shown once. While we focus on the landmarks that are mostly around the nose region, most of it is relevant to research on facial surgeries and facial recognition in general.

Pronasale/Tip (prn) was a landmark that was studied the most, followed by other commonly studied landmarks such as Exocanthion, Cheilion, Endocanthion, Nasion/Radix, Subnasale, Labiale Inferius, Labiale Superius. However, we could not find any pseudocode listed in the literature for the following facial landmarks, and we devised original algorithms for those:

- Alar Base Junction/Alar Crease - left/right
- Alar Rim's Highest Point - left/right
- Columellar Break Point
- Columellar Rim - left/right
- Lateral helix of ear - left/right
- Maxillofrontale - left/right
- Glabella/Menton
- Nasal Parenthesis - left/right
- Nasion/Radix
- Supratip Break Point
- Tip Defining Point - left/right
- Trichion
- Zygion - left/right
- Subalare - left/right
- Subnasale - left/right

We studied the existing algorithms in the literature and implemented either an original algorithm or one similar to the algorithms presented in the literature. We listed the names of the articles that included pseudocode for a facial landmark and the originality of our algorithms in Table 1.

Facial landmark	Articles that have pseudocode for the landmark	Influenced by or original
Alare/Alar Flare - left/right	[Abu, Ngo, et. al. 2019][16], [Vezzetti, Marcolin 2014] [33], [Liang, Wu, et. al. 2013] [19], [Guo, Mei et. al. 2013] [30], [Berretti, Ben Amor, et. al. 2011] [26], [Gupta, Markey, et. al. 2010] [17], [Vezzetti, E., Marcolin, F., Tornincasa, S. et al. 2018] [18], [M. P. Pamplona Segundo, L. Silva, O. R. P. Bellon and C. C. Queirolo] [25].	Influenced by Liang, Wu, et. al. 2013 and Abu, Ngo, et. al. 2019
Cheilion - left/right	[Liang, Wu, et. al. 2013] [19], [Galvánek, Furmanová, et. al. 2015] [37] [Berretti, Ben Amor, et. al. 2011] [26], [Gupta, Markey, et. al. 2010] [17], [Vezzetti, E., Marcolin, F. 2014] [33].	Original
Endocanthion - left/right	[Vezzetti, Marcolin 2014] [33], [Liang, Wu, et. al. 2013] [19], [Berretti, Ben Amor, et. al. 2011] [26], [Galvánek, Furmanová, et. al. 2015] [37] [Gupta, Markey, et. al. 2010] [17], [Moos, Marcolin, et. al. 2017] [34], [Vezzetti, E., Marcolin, F., Tornincasa, S. et al. 2018] [18], [M. P. Pamplona Segundo, L. Silva, O. R. P. Bellon and C. C. Queirolo] [25].	Original
Exocanthion - left/right	[Vezzetti, Marcolin 2014] [33], [Liang, Wu, et. al. 2013] [19], [Berretti, Ben Amor, et. al. 2011] [26], [Galvánek, Furmanová, et. al. 2015] [37] [Gupta, Markey, et. al. 2010] [17] [Vezzetti, E., Marcolin, F., Tornincasa, S. et al. 2018] [18], [M. P. Pamplona Segundo, L. Silva, O. R. P. Bellon and C. C. Queirolo] [25].	Original
Gnathion	[Manal, Arsalane, et. al. 2019] [5]	Original
Labiale Superius	[Abu, Ngo, et. al. 2019] [16], [Manal, Arsalane, et. al. 2019] [7], [Vezzetti, E., Marcolin, F. 2014] [33].	Influenced by Abu, Ngo, et. al. 2019
Pronasale/Tip	[Abu, Ngo, et. al. 2019] [16], [Vezzetti, Marcolin 2014] [33].	influenced by Abu, Ngo, et. al. 2019
Sellion	[Liang, Wu, et. al. 2013] [19].	influenced by Liang, Wu, et. al. 2013
Stomion	[Abu, Ngo, et. al. 2019] [16], [Manal, Arsalane, et. al. 2019] [7], [Galvánek, Furmanová, et. al. 2015] [37].	influenced by Abu, Ngo, et. al. 2019
Subnasale	[Abu, Ngo, et. al. 2019] [16], [Vezzetti, Marcolin 2014] [33], [Liang, Wu, et. al. 2013] [19], [Guo, Mei et. al. 2013] [30], [Moos, Marcolin, et. al. 2017] [34], [Vezzetti, E., Marcolin, F., Tornincasa, S. et al. 2018] [18],	Influenced by Guo, Mei et. al. 2013

The implementations were done in Python (version 3.1), and Trimesh Python library was used to load 3D models that are in Wavefront (.obj) format. The algorithms assume that the face 3D models are placed in the correct pose and orientation on the x , y , and z coordinate systems, facing the z -axis.

The algorithms utilize the geometric properties of the head to find landmark locations, and most of the algorithms depend on finding the location of another landmark. Once the location of the other landmark(s) is found, some facial statistics (mean and standard deviation) of distances between landmark locations are utilized to determine the location of the landmark. The statistics are mostly retrieved from facebase.org's 3D facial norm database. For various algorithms, we could not find measurement statistics at facebase.org about the landmarks that will help us guide our algorithms. For those, we calculated statistics based on our proprietary 3D model dataset that includes 115 3D facial scans of adults. The list of the statistics used while locating the landmarks and the dependent landmarks that need to be located before the landmark are listed in Table 2. Figure 2 depicts the hierarchy of dependencies between the landmarks. As shown in Figure 2 (and in Table 2), almost all algorithms utilize the location of Pronasale, and many algorithms depend on locating Subnasale.

TABLE 2

Facial Landmark	Dependent Landmarks	Source of Statistics
Alar Base Junction/Alar Crease - left/right	Alar flare, Subnasale	Facebase
Alar Rim's Highest Point - left/right	Subnasale	Proprietary dataset
Alare/Alar Flare - left/right	Pronasale, Subnasale	Facebase
Cheilion - left/right	Stomion, Alar flare	Facebase
Columellar Break Point	Pronasale	Proprietary dataset
Columellar Rim - left/right	Pronasale	Proprietary dataset
Endocanthion - left/right	Sellion	Facebase
Exocanthion - left/right	Sellion	Facebase
Glabella	Pronasale	Facebase
Labiale Superius	Subnasale	Facebase
Lateral helix of ear - left/right	N/A	Facebase
Maxillofrontale - left/right	Pronasale, Endocanthion	Proprietary dataset
Menton/Gnathion	Pronsasale	Facebase
Nasal Parenthesis - left/right	Pronasale	Proprietary dataset
Nasion/Radix	Pronasale	Facebase
Pronasale/Tip	N/A	N/A
Sellion	Pronasale	Facebase
Stomion	Labiale Superius	Facebase
Subalare - left/right	Subnasale	Facebase, Proprietary dataset
Subnasale - left/right	Subnasale	Proprietary dataset
Subnasale	Pronasale	Facebase
Supratip Break Point	Pronasale	Proprietary dataset
Tip Defining Point - left/right	Pronasale	Proprietary dataset
Trichion	Glabella	Proprietary dataset
Zygion - left/right	Pronasale	Facebase, Proprietary dataset

FIGURE 2.

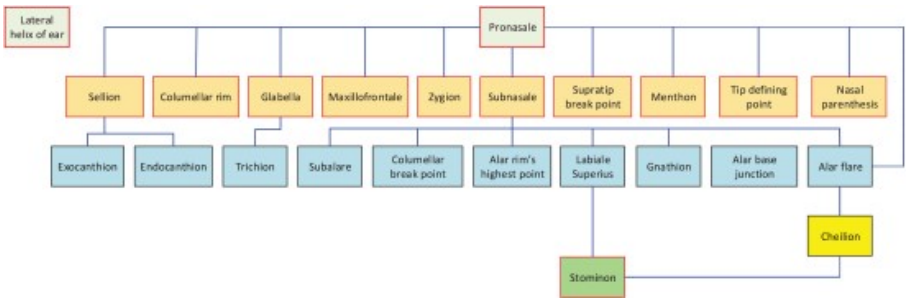

PSEUDOCODE FOR LANDMARK DETECTION

CHAPTER III

In this section, we present the description of the landmarks and their pseudocode:

A. Alar Flare (ALARE) (Left/Right)

Alar Flare (Alare) is the most lateral point on the left and right ala of the nose.

Pseudocode:

1. Locate the Pronasale and Subnasale.
2. Select all vertices that are above the Subnasale's y-coordinate, and between the Subnasale's z-coordinate and the Pronasale's z-coordinate.
3. Sort the vertices by x-coordinate.
4. Assign the leftmost vertex as the Alar Flare Left.
5. Assign the rightmost vertex as the Alar Flare Right.

B. Alar Base Junction/Alar Crease (Left/Right)

Alar base is the junction between the alar crease and the cheek.

Pseudocode:

6. Find the subnasale.
7. Select vertices slightly above and to the left of the subnasale based on the subnasal width statistics
8. Sort the vertices by x
9. Assign the vertex with a relative z minima as the left subalare
10. Select vertices slightly above and to the right of the subnasale based on the subnasal width statistics
11. Sort the vertices by x
12. Assign the vertex with a relative z minima as the right subalare

C. Alar Rim's Highest Point (Left/Right)

The highest point of the left alar rim.

Pseudocode:

13. Find the subnasale
14. Select vertices diagonal-left above the subnasale using Nasal Width (Right Alare (al_r) to Left Alare (al_l)) statistical data from facebase.org
15. Sort the vertices multidimensionally using both x and y in quadrant 1, i.e. sort by x + y
16. Assign the uppermost x and y vertex as the left alar rim's highest point
17. Select vertices diagonal-right above the subnasale using Nasal Width (Right Alare (al_r) to Left Alare (al_l)) statistical data from facebase.org
18. Sort the vertices multidimensionally using both x and y in quadrant 4, i.e. sort by x - y

Assign the uppermost x and y vertex as the right alar rim's highest point.

D. Cheilion (Left/Right)

Cheilion is the landmark located at the oral commissure where the upper and lower lips meet on left/right side of the gently closed lips.

Pseudocode:

19. Find the stomion.
20. Select vertices on the left of the stomion with similar x -values based on the Labial Fissure Width statistics.
21. Find a vertex with a relative z minimum or a z -value lower than the stomion.
22. Assign this vertex as the left cheilion.
23. Select vertices on the right of the stomion with similar x -values based on the Labial Fissure Width statistics.
24. Find a vertex with a relative z minimum or a z -value lower than the stomion.
25. Assign this vertex as the right cheilion.

E. Columellar Rim (Left/Right)

They are the lowest points (or widest points) of the left and right nostrils, as seen from the lateral view on the columellar side at the mucocutaneous junction.

Pseudocode:

26. Find the pronasale.
27. Select vertices diagonally downwards to the left of the pronasale using statistical data from proprietary dataset.
28. Sort the vertices by both x and y coordinates, using quadrant 4 (i.e., sort by x - y).
29. Assign the last vertex as the left columellar rim.
30. Select vertices diagonally downwards to the right of the pronasale using statistical data from proprietary dataset.
31. Sort the vertices by both x and y coordinates, using quadrant 1 (i.e., sort by x+y).
32. Assign the first vertex as the right columellar rim.

F. Columellar Break Point

Columellar break point is the point in the columellar region of the nose where the tip of the nose stops curving, and the columellar linear structure begins, in the midline.

Pseudocode:

33. Find the subnasale.
34. Select vertices above the subnasale using statistical data.
35. Sort the vertices by y .
36. Assign the largest y as the columellar break point.
37.

G. Endocanthion (Left/Right)

Endocanthion is the inner corners of the eye where the upper and lower eyelids meet. In the literature, it is also known as Medial Canthus.

Pseudocode:

38. Find the sellion
39. Starting from the sellion, select vertices to the left in a region defined based on the 'Intercanthal Width' statistics from facebase.org's 3D norms database.
40. First, select a region that is away by the mean value of 'Intercanthal Width' from the sellion. If a local minimum is not found, expand the region by standard deviation of 'Intercanthal Width' at each iteration.
41. When the vertex that satisfies the local minima condition (x value

is larger than next two vertices and smaller then previous two vertices) is found, assign this vertex as the left endocanthion.
42. Repeat the same process in the opposite direction to find the right endocanthion.

H. Exocanthion (Left/Right)

Exocanthion is the outer corner of the eye where the upper and lower eyelids meet. In the literature, it is also known as Lateral Canthus.

Pseudocode:

43. Find the sellion.
44. Starting from the sellion, select vertices to the left in a region defined based on the 'Outercanthal Width' statistics from facebase.org's 3D norms database.
45. First, select a region that is a certain distance from the sellion, based on the mean value of 'Intercanthal Width'. If a local minimum is not found, expand the region by the standard deviation of 'Outercanthal Width' at each iteration.
46. When a vertex that satisfies the local minimum condition (its x value is larger than the next two vertices and smaller than the previous two vertices) is found, assign it as the left exocanthion.
47. Repeat the same process in the opposite direction to find the right exocanthion.

I. Glabella

Glabella is the most prominent point of the forehead in the midline between the eyebrows.

Pseudocode:

48. Find the pronasale.
49. Select vertices above the pronasale.
50. Assign the vertex with a relative maximum z-value as the glabella.

J. Gnathion (Menton)

Gnathion (menton) is the lowest point on the soft tissue profile of the chin in mid-sagittal plane.

Pseudocode:

51. Find the pronasale
52. Select vertices based on the stats from facebase.org that gives the distance between the pronasale and gnathion: [lower face height + nasal height - nasal bridge length].
53. Find the lowest relative maxima for z.
54. Assign this vertex as the gnathion.

K. Labiale Superius

Labiale superius is the midline point representing the mucocutaneous vermilion border of the upper lip.

Pseudocode:

55. Find the subnasale.
56. Select vertices below the subnasale based on the Philtrum Length statistics from the selection region, which will be determined by the mean value of Philtrum Length.
57. Find the vertex with a relative maximum for the z -coordinate.
58. If a vertex with a relative maximum for z cannot be found, expand the region by one standard deviation of Philtrum Length.
59. When a vertex with a relative maximum for z is found, assign it as the labiale superius.

L. Lateral Helix of Ear (Left/Right)

The helix of ear (left/right) is the utmost point on the helix of the left ear.

Pseudocode:

60. Use the minimum and maximum y-values of the vertices, along with the statistics of nasal bridge length, to find the region along the y -axis that will include the lateral helix of the ear.
61. Within this region, find the vertex with the largest x -value within one standard deviation from the midpoint.
62. Assign this vertex as the left lateral helix.
63. Within this region, find the vertex with the smallest x-value within one standard deviation from the midpoint.
64. Assign this vertex as the right lateral helix.

M. Maxillofrontale (Left/Right)

Maxillofrontale is the point where the maxilloanterioral and nasoanterioral sutures meet.

Pseudocode:

65. Find the pronasale and endocanthion.
66. Select vertices at the y -coordinate level of the endocanthion and to the left of the pronasale using statistics from proprietary dataset.
67. Sort the vertices by x -coordinate.
68. Assign the last vertex as the left maxillofrontale.
69. Select vertices at the y -coordinate level of the endocanthion and to the right of the pronasale using statistics from proprietary dataset.
70. Sort the vertices by x -coordinate.
71. Assign the first vertex as the right maxillofrontale.

N. Nasal Parenthesis-Left/Right

Nasal parenthesis is the summit of the left/right nasal parentheses/canthal-alar line.

Pseudocode:

72. Find the pronasale.
73. Select vertices diagonally upwards to the left of the pronasale using statistics from proprietary dataset.
74. Sort the vertices by both x and y coordinates, using quadrant 1 (i.e., sort by x+y).
75. Assign the last vertex as the left nasal parenthesis.
76. Select vertices diagonally upwards to the right of the pronasale using statistics from proprietary dataset.
77. Sort the vertices by both x and y coordinates, using quadrant 4 (i.e., sort by x - y).
78. Assign the first vertex as the right nasal parenthesis.

O. Nasion (Radix)

Nasion (Radix) is the midpoint of the nasofrontal suture line where the frontal bone and nasal bones join.

In some of the literature, Nasion (Radix) and Sellion are considered the same landmark. There are no geometric properties on the surface of the face that can be utilized to distinguish Nasion from Sellion. Therefore, we accepted Sellion and the Nasion as the same landmark. When the location of Nasion is needed, our implementation calls the function for Sellion and returns the location of the Sellion. Therefore, the pseudocode for Sellion is the same as Nasion. Nasion landmark is not counted for the total landmark count (thirty-eight) in this study.

P. Pronasale (Tip)

Pronasale (tip) is the most protrusive point on the nasal tip in the midline.

Pseudocode:

79. Determine the minimum and maximum x and y coordinates (min_x , max_x , min_y , max_y) of the vertices.
80. Define a region where the nose is approximately centered by calculating the coordinates (center = (min_x+ max_x)/2, y = (min_y+ max_y)/3).
81. Sort the vertices within the defined region and locate the vertex with the highest z value. Assign this vertex as the Pronasale.

Q. Sellion

Sellion is the deepest depression of the nasal bones and often coincides with soft tissue nasion.

Pseudocode:

82. Locate the Pronasale.
83. Starting from the Pronasale, use the nasal bridge length statistics (Nasion (n) to Pronasale (prn)) from facebase.org to establish a search region with one standard deviation of nasal bridge length.
84. Iterate through the search region on the increasing y-axis until a relative minimum for the z-coordinate is found.
85. If a relative minimum is not found in the initial search region, expand the search region by one standard deviation of nasal bridge length.
86. If a relative minimum is found, assign the vertex in the search region as the Sellion.

R. Subnasale

Subnasale is the deepest point at the junction of the base of the columella and the upper lip in the midline.

Pseudocode:

87. Locate the Pronasale.
88. Define the height and depth of the search region based on the Nasal height (Nasion (n) to Subnasale (*sn*)) and Nasal bridge length (Nasion (n) to Pronasale (prn)) statistics, as well as the Nasal Protrusion (Pronasale (prn) to Subnasale (*sn*)) statistics from facebase.org.
89. Search for an inflection point on the z-axis below the y-axis of the Pronasale, in decreasing order. (Note that this algorithm might only work if the y-axis of the Pronasale is less than the y-axis of the Subnasale. Some nose shapes, such as those with a drooping tip, may have this property).
90. Assign this vertex as the Subnasale.

S. Stomion

The point at which the upper and lower lip make contact in the midline on gently closed lips.

Pseudocode:

91. Find the labiale superius
92. Select vertices below the labiale superius based on the Upper Vermilion Height (Labiale Superius (ls) - Stomion (sto)) statistics from facebase.org
93. Find the first vertex with a relative z minima
94. Assign this vertex as the stomion
95.

T. Subalare (Left/Right)

Subalare is the point at the lower limit of each alar base, where the alar base disappears

into skin of the upper lip. It is a bilateral landmark located below the nostril opening at the point where the infero-medial continuation of the alar cartilage inserts into the skin of the upper lip.

Pseudocode:

96. Find the subnasale.
97. Select vertices slightly above and to the left of the subnasale based on the subnasal width statistics.
98. Sort the vertices by x .
99. Assign the vertex with a relative z minima as the left subalare.
100. Select vertices slightly above and to the right of the subnasale based on the subnasal width statistics.
101. Sort the vertices by x .
102. Assign the vertex with a relative z minima as the right subalare.

U. Subnasale (Left/Right):

Subnasale left/right are the points where the right/left columella meets the nostril sill.

Pseudocode:

103. Locate the Subnasale.
104. Select vertices to the left based on the 'subnasale width' (Right Subalare (sbal_r) to Left Subalare (sbal_l)) statistics from facebase.org's 3D norms database. Since the Subnasale is approximately half the distance to the Subalare from the Subnasale, divide the 'subnasale width' by 2.
105. Sort the vertices by increasing x -coordinate.
106. Assign the vertex with the largest x -coordinate as the Subnasale left.
107. Select vertices to the right based on the 'subnasale width' statistics from facebase.org's 3D norms database.
108. Sort the vertices by decreasing x-coordinate.
109. Assign the vertex with the smallest x-coordinate as the Subnasale right.

V. Supratip Break Point

Supratip break point is the area just cephalad to the nasal tip at the caudal portion of the nasal dorsum.

Pseudocode:

110. Find the pronasale.
111. Select vertices above the pronasale using statistics from proprietary dataset.
112. Sort the vertices by y -coordinate.
113. Assign the last vertex as the supratip break point.

W. Tip Defining Point (Left/Right)

The nasal tip defining point is the most anterior projection of the tip cartilages, usually corresponding to the apex of the lobular arch anatomically, and is typically identified

externally where the light reflex is seen on the nasal tip.
Pseudocode:

114. Find the pronasale
115. Select vertices above and to the left of the pronasale using statistics from proprietary dataset.
116. Sort the vertices by *y*- coordinate
117. Assign the last vertex as the left tip defining point.
118. Select vertices above and to the right of the pronasale using statistics from proprietary dataset.
119. Sort the vertices by *y*- coordinate
120. Assign the last vertex as the left tip defining point.

X. Trichion

The trichion is the point on the hairline in the midline of the forehead.
Pseudocode:

121. Find the glabella
122. Select vertices above the glabella between the glabella and trichion based on the statistics
123. Search upwards to find the first vertex that has a significant z increase which indicates the existence of hair.

Y. Zygion (Left/Right)

Zygion is the most lateral point of the right zygomatic arch.
Pseudocode:

124. Find the pronasale.
125. Using the maximum facial width statistics (from right Zygion to left Zygion) from facebase.org, determine the x -coordinate value of the left zygion.
126. Using statistics, determine the y-coordinate value of the left zygion.
127. Select all vertices in the region based on the x and y coordinate values.
128. Sort the vertices by both x and y coordinates, using quadrant 1 (i.e., sort by x+y).
129. Assign the vertex as the left zygion.
130. Using the maximum facial width statistics (from right Zygion to left Zygion) from facebase.org, determine the
131. x -coordinate value of the right zygion.
132. Using statistics, determine the y-coordinate value of the right zygion.
133. Select all vertices in the region based on the x and y coordinate values within a diagonal line to the approximate location.
134. Sort the vertices by both x and y coordinates, using quadrant 4 (i.e., sort by x - y).
135. Assign the vertex as the right zygion.

Results and Discussion
CHAPTER IV

We have tested the algorithms on 111 facial 3D models for thirty-eight landmarks. The temporal analysis of algorithms shows that it takes on average 0.5 seconds to locate a landmark at the first level (e.g. Pronasale), 0.8 seconds to locate a landmark at the second level (e.g. Subnasale), and 1.1 seconds for a landmark at the third level shown in Figure 2 when the algorithm is executed on a Jupyter Notebook page using the Python 3.1 kernel at MacBook Pro with M1 Max Chip and 32GB memory.

We calculate the error by finding the distance between the manual markings and the location found by the algorithm. The mean error for each landmark is calculated using the formula below. In this formula, x_{mi} , y_{mi} , and z_{mi} represent the coordinates of manual markings and x_{ai} , y_{ai} , and z_{ai} represent the coordinates found by the algorithm.

$$1n\sum_{i=1n}(x_{mi}-x_{ai})2+(y_{mi}-y_{ai})2+(z_{mi}-z_{ai})2-----------------------------------\sqrt{}$$

Table 3 presents the mean, median, standard deviation, minimum, and maximum values of the errors for the 111 samples. The values are in millimeters and the table is sorted based on the mean values. The algorithms for bilateral landmarks work with the same logic for the left and right landmarks, and hence their results are very similar. Therefore, we only present the results for the left of the bilateral landmarks.

Facial Landmark	mean	median	std	min	max
Pronasale/Tip	1.98	1.82	1.13	0	5.25
Tip Defining Point-left	3.45	2.84	2.12	0.08	10.64
Supratip Break Point	3.75	3.06	2.44	0.15	11.96
Columellar Break Point	3.87	3.38	2.47	0.18	13.06
Labiale Superius	4.28	3.92	2.21	0.2	10.32
Nasal Parenthesis – left	5.16	4.67	2.81	0.1	14.94
Glabella	5.54	4.98	3.93	0.41	24.88
Subnasale	5.58	5.64	2.1	0.32	11.14
Stomion	5.59	5.41	2.52	1.01	12.99
Endocanthion – left	5.94	5.24	3.23	0.35	14.12
Alare/Alar Flare – left	6.99	6.29	3.94	0.89	21.12
Subnasale – left	7.13	6.53	2.97	1.17	15.55
Alar Rim's Highest Point – left	7.2	6.49	3.74	0.69	18.47
Subalare – left	7.25	7.23	3.51	0.77	15.11
Cheilion – left	8.06	7.81	3.92	0.85	22.27
Zygion – left	8.08	7.35	4.48	0.32	23.43
Exocanthion – left	9.24	8.11	5.1	0.38	24.01
Maxillofrontale – left	10.04	9.58	4.09	1.7	19
Trichion	10.19	7.72	9.12	1.28	52.71
Columellar Rim - left	10.31	10.33	3.1	3.4	19.42
Alar Base Junction - left	11.11	10.9	3.01	3.2	19.49
Sellion	11.4	11.14	4.21	3.23	21.59
Gnathion	11.56	9.41	8.43	0.22	41.21
Lateral helix of ear - left	18.16	12.87	15.8	0	85.63

The mean is almost always larger than the median due to the outliers in the errors. The maximum values in Table 3 -Y indicate the extent of the outliers. We had the most outliers

for the lateral helix of the ear and trichion landmarks. As we investigated the cause, we noticed that the heuristic of the algorithm lateral helix of the ear did not work since the minimum and maximum points on the x-axis were not always the ear on the 3D scan due to hair. We also noticed that the heuristic of the trichion also did not work due to lack of hair or due to hair not being tied back during the 3D scan as the algorithm detects the changes in the z-axis caused by the hair.

Figure 3 provides the histogram of error values to show the distribution of the error values and outliers. According to Figure 3, the largest errors and outliers exist for the lateral helix of the ear, trichion, and gnathion landmarks. The smallest errors exist for the Pronasale, which is a good sign since almost all landmarks depend on detecting the Pronasale first. The Subnasale, which is another landmark that many landmarks depend on, does not have high error.

FIGURE 3.

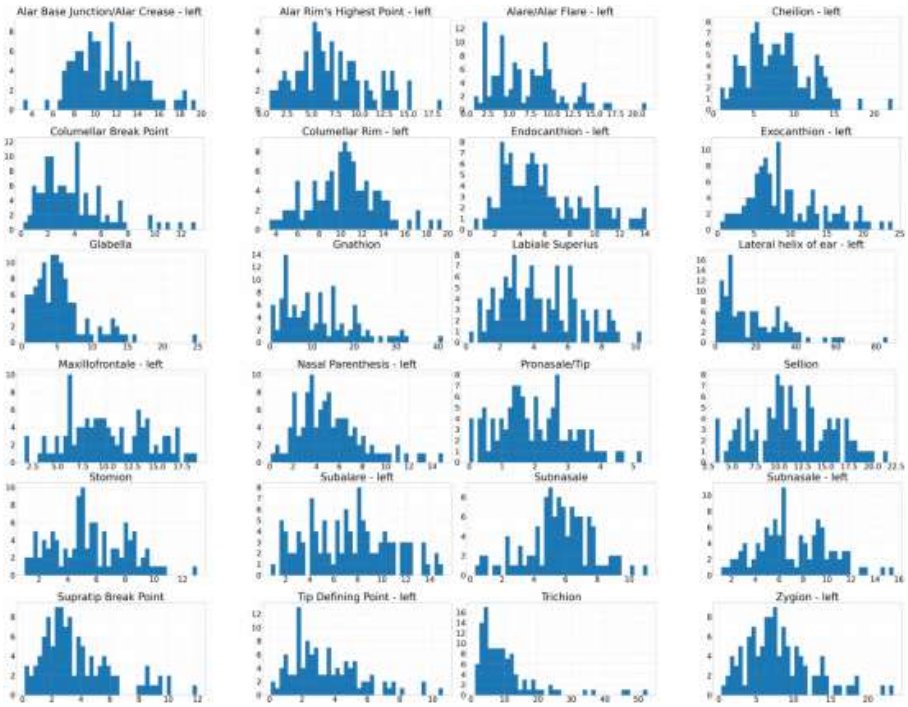

While we compare our results with manual markings, note that manual markings can have errors. The markings can also slightly change from one rater (the person who does the marking) to another, and the reliability of the raters should be tested. To achieve more accurate manual markings, several raters could be utilized, and then the average of the markings could be computed to reach a consensus.

To reduce the results, the utilization of statistics can be extended to incorporate more heuristics. For example, statistics about the average face width and height were utilized to estimate the difference between the x and y coordinates of the Zygion and the Pronasale landmarks.

We could improve this by first determining how wide and long the subject's face is when compared to the average face width and height, and then better estimate the x and y coordinates of the Zygion given the x and y coordinates of the Pronasale utilizing the ratio of the subject's face and the average face values. Similar statistics and heuristics can be utilized for other landmarks based on the ratio of the subject's measurement and the average of that measurement to compute the location of the landmark.

The performance of the algorithms can further be improved if the age, gender, and ethnicity of the subject are known or can be estimated by utilizing statistics for the subject's age, gender and ethnicity.

Conclusion
CHAPTER V.

In this study, we developed algorithms to detect facial landmarks based on geometric properties and facial statistics. Facial landmark detection is widely applied in fields, such as face recognition, face surgery, biometrics, and surveillance systems. We reviewed the pseudocode of algorithms in the current literature. and developed algorithms for thirty-eight landmarks using geometric properties and statistical information about facial measurements. The algorithms for thirty landmarks are original contributions to literature.

To the best of our knowledge, this study covers the largest number of facial landmark detection algorithms based on the geometric properties of 3D models. This is the first study that provides the implementation of the algorithms along with detailed pseudocode.

The results indicate that the geometric properties of the face and the facial statistics can be utilized to discover many landmark locations, and the output of high-performing algorithms, such as Pronasale, can be combined with outputs of other approaches, such as machine learning approaches to provide a more robust solution for facial landmark detection.

ACKNOWLEDGMENT

The authors would like to thank Philip Sawyer, Joshua Palmer, and Aidan Beeching for their help in reviewing the existing erature for the pseudocode of the facial algorithms.

REFERENCES

1. M. Lal, K. Kumar, R. Hussain, A. Maitlo, S. Ali and H. Shaikh, "Study of face recognition techniques: A survey", *Int. J. Adv. Comput. Sci. Appl.*, vol. 9, no. 6, 2018.

2. G. Lekakis, G. Hens, P. Claes and P. W. Hellings, "Three-dimensional morphing and its added value in the rhinoplasty consult", *Plastic Reconstructive Surg.-Global Open*, vol. 7, no. 1, pp. e2063, Jan. 2019.

3. Y. Jing, X. Lu and S. Gao, "3D face recognition: A survey", *arXiv:2108.11082*, 2021

4. S. Zhou and S. Xiao, "3D face recognition: A survey", *Hum.-Centric Comput. Inf. Sci.*, vol. 8, no. 1, Nov. 2018.

5. E. R. Manal, Z. Arsalane and M. Aicha, "Automated detection of craniofacial landmarks on a 3D facial mesh", *Proc. Int. Conf. Integr. Design Prod.*, pp. 537-548, Nov. 2020.